Developmental Biology 398 (2015) 163–176

Contents lists available at ScienceDirect

Developmental Biology

journal homepage: www.elsevier.com/locate/developmentalbiology

Ecdysone regulates morphogenesis and function of malpighian tubules in *Drosophila melanogaster* through EcR-B2 isoform

Naveen Kumar Gautam [a,b], Puja Verma [a], Madhu G. Tapadia [a,*]

[a] Cytogenetics Laboratory, Department of Zoology, Banaras Hindu University, Varanasi 221005,Uttar Pradesh, India
[b] Molecular and Human Genetics Laboratory, Department of Zoology, University of Lucknow, Lucknow 226007, Uttar Pradesh, India

ARTICLE INFO

Article history:
Received 4 February 2014
Received in revised form
20 October 2014
Accepted 11 November 2014
Available online 2 December 2014

Keywords:
Drosophila melanogaster
Malpighian tubules
Ecdysone receptor
Uric acid
Na^+/K^+ ATPase

ABSTRACT

Malpighian tubules are the osmoregulatory and detoxifying organs of *Drosophila* and its proper development is critical for the survival of the organism. They are made up of two major cell types, the ectodermal principal cells and mesodermal stellate cells. The principal and stellate cells are structurally and physiologically distinct from each other, but coordinate together for production of isotonic fluid. Proper integration of these cells during the course of development is an important pre-requisite for the proper functioning of the tubules. We have conclusively determined an essential role of ecdysone hormone in the development and function of Malpighian tubules. Disruption of ecdysone signaling interferes with the organization of principal and stellate cells resulting in malformed tubules and early larval lethality. Abnormalities include reduction in the number of cells and the clustering of cells rather than their arrangement in characteristic wild type pattern. Organization of F-actin and β−tubulin also show aberrant distribution pattern. Malformed tubules show reduced uric acid deposition and altered expression of Na^+/K^+-ATPase pump. B2 isoform of ecdysone receptor is critical for the development of Malpighian tubules and is expressed from early stages of its development.

Introduction

The Malpighian tubules (MTs) of *Drosophila* are renal organs that perform excretory and osmoregulatory functions like kidney in vertebrates and humans. The two pairs of MTs originate from the junction between the midgut and hindgut with one pair migrating anteriorly and the other pair posteriorly. The mature MTs are derived from ectodermal epithelial buds which give rise to the principal cells (PCs) and surrounding mesenchymal mesoderm undergo mesenchymal to epithelial transition as they get integrated and finally differentiate into stellate cells (SCs). The number of these cells remains fairly constant throughout the life (Wessing and Eichelberg, 1978; Sozen et al., 1997; Denholm et al., 2003; Hatton-Ellis et al., 2007; Jung et al., 2005). There are other smaller cells that have now been identified as the stem cells and neuro-endocrine cells (Singh et al., 2007).

Steroid hormone ecdysone is critical for the development of *Drosophila* in all stages starting from embryogenesis to larval molting, pupation and metamorphosis. Ecdysone exerts its effects through a heterodimer of ecdysone receptor (EcR) and ultraspiracle (USP) (Yao et al., 1992; Thomas et al., 1993). *USP* is the *Drosophila* homolog of vertebrate Retinoid X receptor (RXR) (Oro et al., 1990; Henrich et al., 1990), while *EcR* gene encodes three functional isoforms, EcR-A, EcR-B1 and EcR-B2 (Koelle et al., 1991; Talbot et al., 1993). These three isoforms differ at their N-terminal, A/B or activation function-1 (AF-1) regions, but share a common conserved carboxy-terminal harboring the C and D domains referred to as the DNA and ligand binding regions respectively (Mouillet et al., 2001). The unique AF-1 domains of EcR isoforms activate the downstream genes in the cell or tissue specific manner. Mutations that block all three isoforms of EcR lead to embryonic lethality, but mutation that blocks one isoform, affects specific developmental processes (Bender et al., 1997). EcR-A predominantly expresses in imaginal discs that develop into adult specific structures while EcR-B1 predominantly expresses in those larval structures which are destined to die (Schubiger et al., 1998; Cherbas et al., 2003; Davies et al., 2005). Due to the absence of EcR-B2 specific mutations, the function of this isoform is less well understood. Ectopic expression of wild type EcR can rescue *EcR* mutant phenotypes depending upon the EcR isoform involved (Cherbas et al., 2003).

Drosophila being a holometabolous insect undergoes complete metamorphosis during pupation, converting the larval life form to the highly motile adult. Metamorphosis is accomplished by the destruction of larval structures and formation of adult structures from specific imaginal cells that have remained quiescent during the entire larval. The destruction of larval and differentiation of adult structures is guided by the steroid hormone, ecdysone. The

* Corresponding author.
E-mail address: madhu@bhu.ac.in (M.G. Tapadia).

http://dx.doi.org/10.1016/j.ydbio.2014.11.003
0012-1606/

Table 1
Over expression of *EcR-DN* under *c42* Gal4 driver causes larval lethality at 1st instar and co-expression of wild type *EcR* isoforms rescue these lethal phenotype to different extents.

Genotype	Embryos	Unfertilized embryos	Total fertilized embryos	Dead embryos	1st instar larvae	Pupae	Flies emerged
WT	1190	115	1075	21	1054	1048	1044 (97.1 %)*
c42 > EcR-DN	1250	152	1098	43	1055	0	0
c42 > EcR-DN; EcR-A	1730	290	1440	36	1404	0	0
c42 > EcR-DN; EcR-B1	1610	53	1557	49	1508	1440	256 (16.4 %)*
c42 > EcR-DN; EcR-B2	1696	126	1570	47	1523	1431	1408 (89.7 %)*

* Percentage of total number of flies emerged.

larval MTs are one of the structures that escape ecdysone induced destruction and are carried over to the adults. In one of the studies we have shown that the proteins involved in the apoptotic pathways are expressed in the MTs but they are not activated due to their sequestration in the nucleus (Shukla and Tapadia, 2011) thus helping them to evade ecdysone induced destruction. Pro-apoptotic proteins are also shown to have a role in the development of MTs (Tapadia and Gautam, 2011). Ecdysone signaling is also important for the integration of SCs in the MTs and Drip expression (Gautam and Tapadia, 2010).

MTs are the excretory organs that remove nitrogenous wastes from the blood and function in osmoregulation (Dow et al., 1994, 1998). The primary function of MTs is secretion of isotonic fluid, which is accomplished by concerted action of physiologically distinct PCs and SCs (Denholm et al., 2003). PCs are enriched with vacuolar-H^+-ATPase transporter which uses Na^+/H^+ and K^+/H^+ exchanger to transport cations into the lumen (O'Donnell et al., 1996) while SCs have ion channels which permit flow of Cl^- ions (O'Donell et al., 1998) and aquaporins which permit water flow into the lumen (Kaufmann et al., 2005). (Na^+/K^+)-ATPase is a transmembrane channel protein expressed exclusively in PCs and is conserved from lower to higher organism and plays an important function in regulation of ionic balance in the cells (Lebovitz et al., 1989). Recently it has been shown that (Na^+/K^+)-ATPase plays an essential role in epithelial immune response in *Drosophila* Malpighian tubules (Verma and Tapadia, 2014).

In this paper we show that disruption of ecdysone signaling in the PCs affected both PCs and SCs, leading to improper development and function of the tubule. A reduction in size of the tubules accompanied by reduced number of PCs and SCs was observed. The functioning of the tubules was also affected due to ionic imbalance resulting in reduced uric acid deposition. Disruption of ecdysone signaling also affected cytoskeletal proteins, F-actin and β-tubulin in the MTs. These phenotypes could be rescued maximally by co-expression of wild type EcR-B2 isoform. Consequently we showed that during early developmental stages, only EcR-B2 is expressed in the MTs but neither EcR-B1 nor EcR-A, suggesting that ecdysone probably mediates its effects through EcR-B2 in the MTs.

Results

Disruption of ecdysone receptor in MTs leads to abnormal development of tubules

To examine the role of ecdysone signaling in the PCs of MTs, we blocked the functioning of endogenous EcR by expressing dominant negative EcR proteins, EcR^{F645A} (EcR-DN), which has mutation in the ligand binding domain, thus affecting all isoforms of EcR (Cherbas et al., 2003). The EcR-DN heterodimerises with USP and binds to ecdysone response elements but does not activate the target gene expression. EcR-DN was expressed in the PCs of MTs using *c42* Gal4 driver (Rosay et al., 1997). *c42* expresses in the PCs of MTs and salivary glands from embryonic stage (Figure S1). EcR-DN expression in salivary glands during embryonic and early larval stages does not hamper with normal development (data not shown) hence we conclude that the phenotypes observed were entirely due to its expression in MTs.

Progenies of *c42 > UAS-EcR-DN* showed delayed development and resulted in early larval lethality (Table 1). The *c42 > EcR-DN* larvae appeared smaller in size (Fig. 1X B) when compared to the wild type (WT) larvae of the same age (Fig. 1X A). The stage of lethality of *c42 > EcR-DN* progeny was determined to be early 1st instar by the mouth-hooks (Fig. 1X B″, blue arrow). These larvae were slow moving (Movie S1) and showed gross abnormalities like low adipose tissue (Fig. S2), transparent cuticle and deformed MTs. The MTs of *c42 > EcR-DN* dying/dead larvae (Fig. 1X B′) were smaller when compared to wild type (Fig. 1X A′). These tubules were not properly elongated in the body cavity and remain coiled. Since, the MTs appeared thin, the external diameter of these tubules was measured and compared to WT. The mean diameter of the main segment of anterior and posterior MTs in the WT larvae was 21 ± 2.1 and 21 ± 2.4 μm respectively while in *c42 > EcR-DN* it was 09 ± 2.4 and 11 ± 1.9 μm respectively. Statistical analysis showed that the mean diameter of MTs in *c42 > EcR-DN* larvae was significantly reduced when compared to wild type (Table 2).

Supplementary material related to this article can be found online at http://dx.doi.org/10.1016/j.ydbio.2014.11.003.

Disruption of ecdysone signaling in PCs leads to reduced cell number and aberrant distribution in tubules

Since disruption of ecdysone receptor in *c42 > EcR-DN* progeny, resulted in smaller tubules, we counted the number of PCs and SCs in these tubules. For an unambiguous identification of cell types, teashirt and cut antibodies were used to identify SCs and PCs respectively (Jung et al., 2005; Singh et al., 2007). Data in Table 3 shows reduction in the number of SCs and PCs in anterior and posterior MTs as compared to wild type. In wild type, the mean number of PCs and SCs in the anterior tubules was 145 ± 1 and 33.2 ± 0.4 respectively while in posterior tubules it was 111.1 ± 1 and 22 ± 0.4 respectively (Sozen et al., 1997). However in *c42 > EcR-DN* larvae, the mean number of PCs and SCs in the anterior tubules was 98.2 ± 3.953 and 23.1 ± 0.9 respectively while in posterior tubules it was 74.4 ± 2.2 and 16.6 ± 0.5 respectively (Table 3). We also looked at the arrangement of these cells after ecdysone disruption in PCs and observed that the regular distribution of PCs as well as SCs (Fig. 1Y B) was altered when compared with the characteristic distribution in wild type (Fig. 1Y A). The number of clusters and cells in each cluster was counted and compared to wild type. It was observed that total number of clusters of PCs and SCs in *c42 > EcR-DN* larvae were significantly more than that in wild type and the number of cells in each cluster was also more as compared to wild type (Table S1). It was observed that disruption of ecdysone in PCs affected both the cell types, which was in contrast to our earlier report that disruption of ecdysone signaling in the SCs, only affected the SCs but not the PCs (Gautam and Tapadia, 2010). The role of

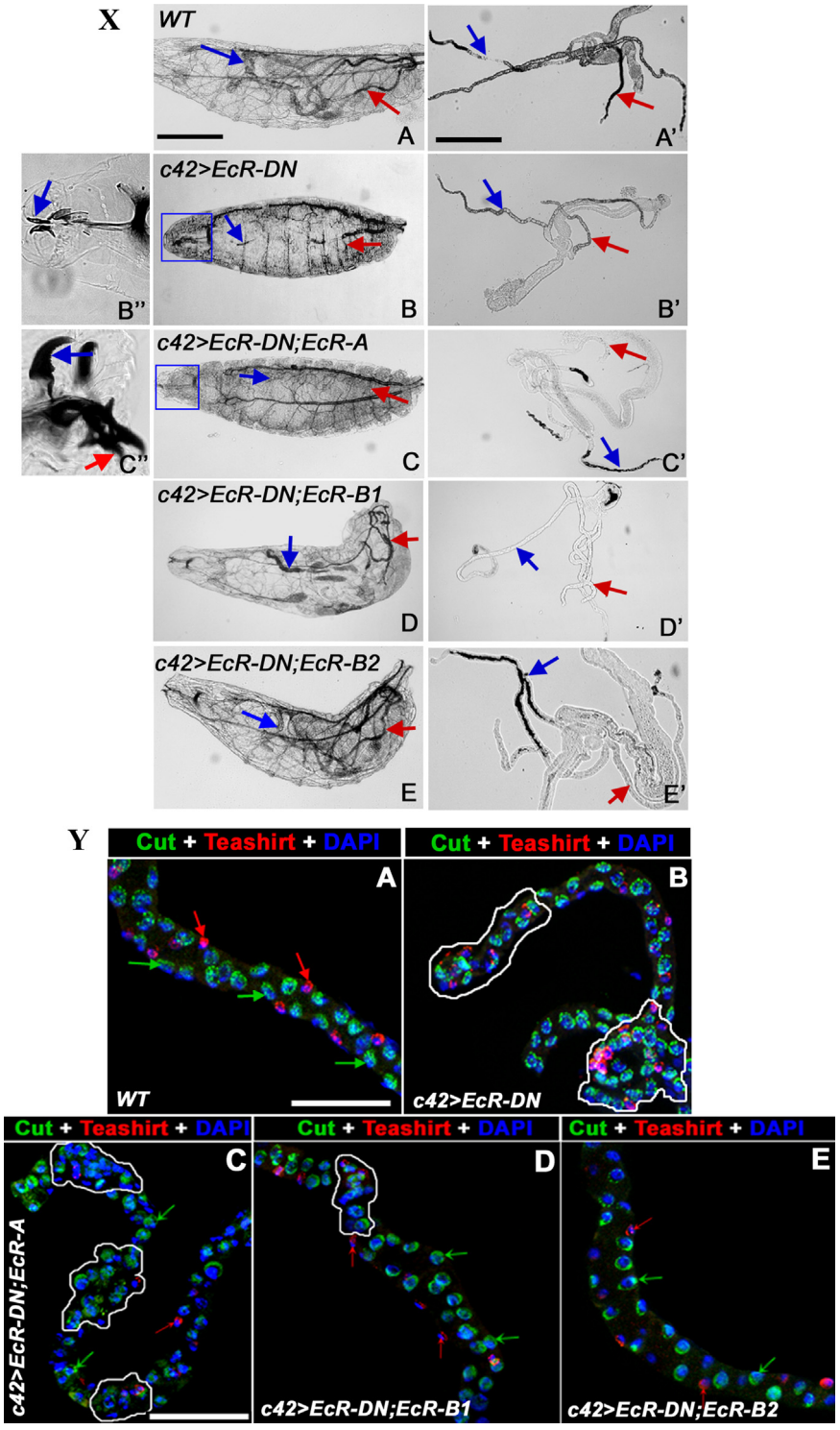

Fig. 1. Disruption of ecdysone signaling in PCs leads to larval lethality, abnormal tubule development and irregular cells arrangements. X. Disruption of ecdysone signaling in *c42 > EcR-DN* larvae show gross developmental abnormalities (B) compared to *WT* (A). The mouth-hooks of dead/dying larvae (B″) show the stage of lethality to be at 1st instar, (B″, blue arrow). Anterior (blue arrow) and posterior (red arrow) MTs of *c42 > EcR-DN* (B) larvae were not properly developed and they were smaller compared to wild type (A′). On co-expression of EcR-A isoform, embryos survived till 2nd instar larval stage (C) and they die during molting as observed by the presence of 2nd (red arrow) and 3rd instar mouth-hook (blue arrow). EcR-B1 and EcR-B2 isoforms rescues lethality till adult flies. Co-expression of EcR-A isoform rescues tubule development to a lesser extent (C′) as compared to EcR-B1 (B′), while EcR-B2 rescues MTs phenotype (E) similar to wild type (Scale bars 100 μm). Y. Irregular arrangement of PCs (green arrows) and SCs (red arrows) in the MTs of *c42 > EcR-DN* (B) compared to wild type (A). Co-expression of EcR-A (C) was not able to restore the arrangement of cells and it remained like *c42 > EcR-DN* (B). EcR-B1 (D) improves it partially while EcR-B2 isoform restores the arrangement maximally (E) and almost same as wild type (A). PCs and SCs were identified by marker protein Cut (green) and Teashirt (red) respectively. DAPI was used as a counter stain for chromatin (Scale bar 20 μm).

ecdysone in MTs development was confirmed using temperature sensitive *ecd*^{1} mutants grown at 29 °C which were also less mobile and had transparent body, low adipose tissue and improperly developed MTs. The MTs were smaller in size and similar to *c42 > EcR-DN* progeny (Fig. 2H). The number of PCs and SCs was reduced and clustered in *ecd*^{1} mutant grown at 29 °C (Fig. 2M and N)

Table 2
Mean (± S.E.) external diameter (in μm) of MTs is reduced by expression of *EcR-DN* transgene and consequently rescued by co-expression of different EcR isoforms.

Genotype ($N=25$)	Anterior tubule	Posterior tubule
WT	21 ± 2.1	21 ± 1.3
c42 > EcR-DN	09 ± 2.4*	11 ± 2.7*
c42 > EcR-DN;EcR-A	11 ± 2.7*	10 ± 1.5*
c42 > EcR-DN;EcR-B1	16 ± 2.3*	15 ± 1.8*
c42 > EcR-DN;EcR-B2	19 ± 2.2	19 ± 1.4

(*N* shows number of tubules measured in each case. *The mean diameter is significant at $P<0.05$. Dunnet's *t*-test was performed with wild type as a control).

Table 3
Co-expression of EcR isoforms were able to restore the reduced number of PCs and SCs in *c42 > UAS EcR-DN* larvae

Genotype ($N=30$)	Anterior tubules		Posterior tubules	
	Principal cells (PCs)	Stellate cells (SCs)	Principal cells (PCs)	Stellate cells (SCs)
WT	144.0 ± 0.4	31.2 ± 0.2	109.1 ± 0.3	21.7 ± 0.1
C42 > EcR DN	98.2 ± 3.9*	23.1 ± 0.9*	74.4 ± 2.2*	16.6 ± 0.5*
c42 > EcR DN; EcR-A	111.2 ± 2.9*	27.2 ± 0.5*	76.0 ± 2.5*	16.4 ± 0.5*
c42 > EcRDN; EcR-B1	128.8 ± 1.9*	28.0 ± 0.5*	100.6 ± 1.5*	19.0 ± 0.4*
c42 > EcR DN; EcR-B2	136.4 ± 1.8	29.1 ± 0.5	103.2 ± 1.5*	19.8 ± 0.4*

N shows the number of tubule counted ($P<0.05$). Dunnett's *t*-test was performed with wild type as a control.

* Significantly reduced number of PCs and SCs compare to wild type.

while in *ecd*[1] grown at 25 °C it was similar to wild type (data not shown). It was also observed that PCs and SCs were not regularly distributed as in wild type.

Co-expression of EcR-B2 isoform rescues phenotypes induced by disruption of ecdysone receptor in MTs

Having observed that expression of EcR-DN with *c42* Gal4 driver causes lethality and disrupted MTs morphology, further investigations were carried out to know which isoform transduces ecdysone signaling. Wild type EcR isoforms were co-expressed individually along with EcR-DN using the same Gal4 driver. To confirm whether bringing extra UAS promoter does not affect the Gal4 titer, we co-expressed EcR-DN;UAS-GFP with the same Gal4 which confirmed that there was no titration of Gal4 driver. It was also observed that *c42 > EcR-DN;UAS-GFP* and *c42 > EcR-DN* larvae showed lethality at similar age (data not shown).

Each of the different EcR isoforms when expressed with EcR-DN was able to rescue the phenotypes but to different extents. Maximum rescue was observed with co-expression of EcR-B2 resulting in 89.7 % adults. These rescued flies were viable and fertile similar to wild type. Co-expression of EcR-B1 resulted in 16.4% adults, remaining died at the pupal stage, however, co-expression of EcR-A could rescue the lethality only up to 2nd instar larval stage (Table 1) and these larvae died at 2nd/3rd instar transition stage (Fig. 1X C and C″). Cuticle preparation of these larvae showed molting defects as 2nd and 3rd instar mouth hooks were both present (Fig. 1X C″). We then observed the MTs and arrangement of cells in each of these rescued progenies. The MTs of viable *c42 > EcR-DN;EcR-B2* (Fig. 1X E′) and E*cR-B1* larvae (Fig. 1X D′) were similar to that of wild type (Fig. 1X A′) while MTs of *c42 > EcR-DN;EcR-A* were not (Fig. 1X C′). The thickness of MTs was measured to confirm this observation which showed that the mean diameter (in μm) of anterior and posterior MTs of *c42 > EcR-DN;EcR-A*, *c42 > EcR-DN;EcR-B1* and *c42 > EcR-DN;EcR-B2* larvae were 11 ± 2.7 and 10 ± 1.5, 16 ± 2.3 and 15 ± 1.8, 19 ± 2.2 and 19 ± 1.4 respectively (Table 2). Statistical analysis did not show significant differences in the thickness of *c42 > EcR-DN;EcR-B2* MTs compared to wild type while, *c42 > EcR-DN;EcR-B1* and *c42 > EcR-DN;EcR-A* larval MTs were significantly reduced. Co-expression of EcR-B2 was able to restore the arrangement of PCs and SCs (Fig. 1Y E) similar to wild type (Fig. 1Y A), while EcR-B1 isoform was also able to restore to certain level (Fig. 1Y D) and EcR-A (Fig. 1Y C) was least efficient.

The restoration of normal arrangement was also measured by counting the number of clusters. Co-expression of EcR-B2 isoform reduced the number of cluster of PCs and SCs to a great extent which was similar to wild type. On the other hand, upon co-expression of EcR-B1 the number of clusters decreased, but not to the same extent as EcR-B2. EcR-A proved to be least efficient in restoring the number of clusters (Table S1). It was also observed that the range of cells in each cluster of PCs and SCs in anterior tubules and posterior tubule were restored to maximum extent in *c42 > EcR-DN;EcR-B2* then *c42 > EcR-DN;EcR-B1* and least in *c42 > EcR-DN;EcR-A* (Table S1).

Next, the number of PCs and SCs were also counted to find out whether the expression of different isoforms was able to restore the cell number. Like other parameters, the different isoforms rescued cell numbers to different extents. The number of PCs, SCs in anterior and posterior tubule of *c42 > EcR-DN;EcR-B2, c42 > EcR-DN;EcR-B1* and *c42 > EcR-DN;EcR-A* were 136.4 ± 1.8, 29.1 ± 0.5 and 103.3 ± 1.5, 19.8 ± 0.4; 111.2 ± 2.9, 27.2 ± 0.6 and 76.0 ± 2.5, 16.4 ± 0.5; 128.8 ± 1.9, 28 ± 0.5 and 100.6 ± 1.5, 19.0 ± 0.4 respectively (Table 2). The above data suggested that EcR-B2 appeared to be most efficient in restoring cell number in MTs followed by EcR-B1, while EcR-A was least efficient.

Expression of EcR-A, B1 and B2 in MTs

As we observed that the expression of EcR-B2 to be most effective in rescuing developmental defects caused by EcR-DN, we wanted to assay the expression of different isoforms in MTs during development. Expression of EcR-A and B1 was observed with respective antibodies during embryonic and larval stages.

The results showed that EcR-A (Fig. 3A) and EcR-B1 (Fig. 3D) do not express in the MTs of embryos (stages 14–15) and appeared same as negative control (not shown). The MTs were identified in the embryos by staining with Cut (Fig. 3B and E, white arrows). Having observed the absence of EcR-A and EcR-B1 in the embryos, immunostaining was done in 1st and 3rd instar larval MTs. Similar to embryos, expression of EcR-A and B1 was not observed in 1st instar larvae (Fig. 3 G and K), but unlike embryos and 1st instar larvae, in wandering 3rd instar larvae, EcR-A expression was observed in the nucleus and cytoplasm (Fig. 3 I), while EcR-B1 expression was observed only in the nucleus (Fig. 3M). Merged images showed the overlay of Cut and DAPI (Fig. 3C and F) and EcR and DAPI (Fig. 3H, J, L and N). These results suggested that EcR-A and B1 do not express during early development but the expression begins in late developmental stages. EcR-B2 analysis could not be performed by immunostaining as EcR-B2 specific antibodies were not available.

To confirm immunostaining results and to know the expression of EcR B2, RT-PCR analysis was performed. Specific primers were designed from unique AF-1 domains of EcR isoformsand used for EcR-A, B1 and B2 transcripts. The sizes of the amplified fragments of EcR-A, B1 and B2 were the 527, 802, 1458 bp respectively (Fig. S3). Similar to immunostaining, no amplification was observed for EcR-A and B1 from RNA of 1st instar MTs, confirming the absence of expression of EcR-A and B1 at 1st instar stages. However, amplification of EcR-B2 was observed in 1st instar larvae suggesting that only EcR-B2 isoform expressed in MTs during early stages (Fig. 3A′). The

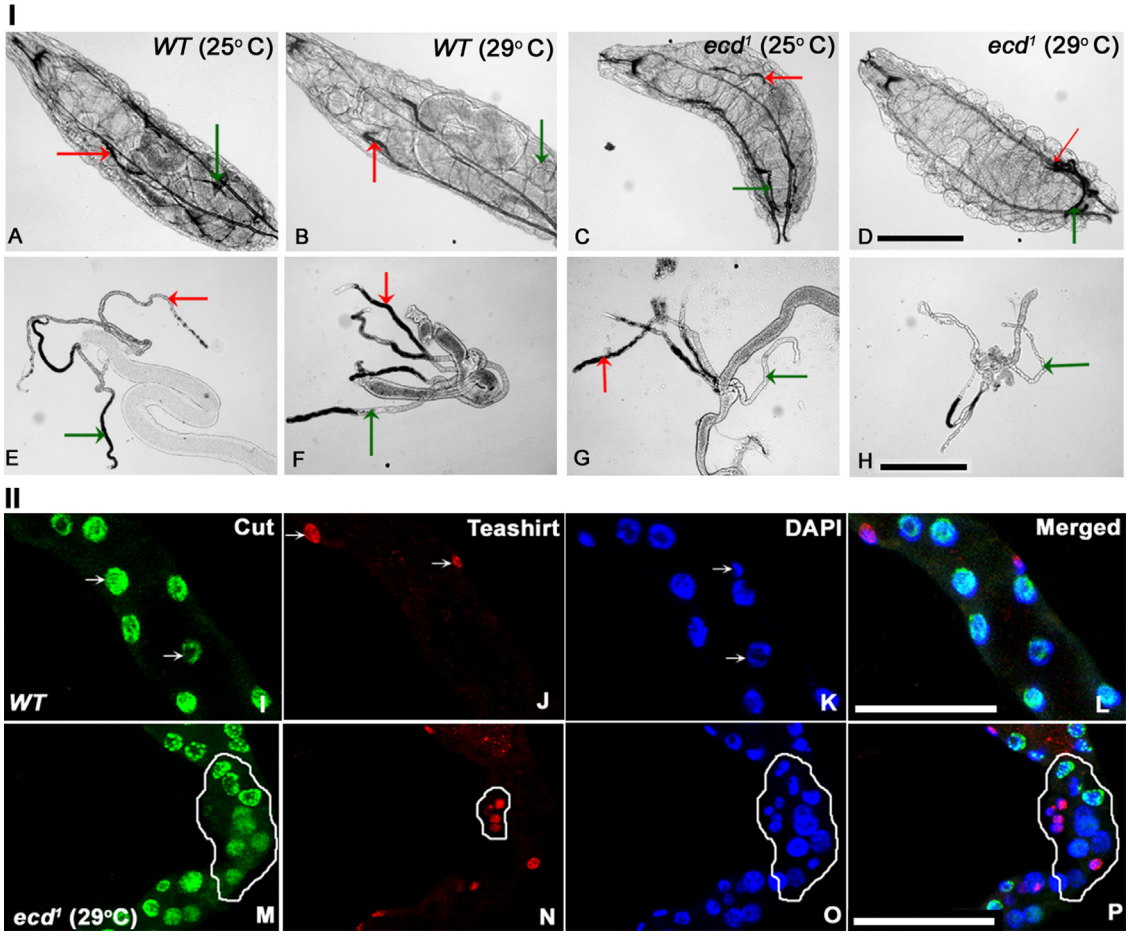

Fig. 2. Disruption of ecdysone signaling in *ecdysoneless* mutant leads to smaller larva and abnormal tubule development. [I] Temperature sensitive ecdysoneless mutant, *ecd*^{1} grown at 29 °C shows developmental delay (D) and abnormal MTs formation (H) while *ecd*^{1} grown at 25 °C shows normal development (C) and MTs (G) similar to WT. Wild type larvae grown at 29 °C (B) develop faster in comparison of wild type larvae grown at 25 °C (A). MTs (F) of wild type larvae grown at 29 °C were normal and similar to those grown at 25 °C (E). (Scale bar 100 μm). [II] *ecd*^{1} grown at 29 °C shows clustering of PCs (M, encircled area) and SCs (N, encircled area) in MTs in comparison to properly arranged PCs (I) and SCs (J) in wild type. DAPI (K, O) staining identifies PCs on the basis of larger nuclei and SCs with smaller nuclei. Merged (L, P) shows the overlay of Cut (I, M), Teashirt (J, N) and DAPI (K, O). PCs (Green, I, M) and SCs (Red, J, N) were identified by marker protein Cut and Teashirt respectively. (Scale bar 20 μm).

amplified EcR-B2 fragment was eluted and labeled to use as probe for DNA–RNA in situ hybridization in embryos and larval MTs. Embryos of stage 13–14 and 15-16 were taken for study as MTs develops during these stages. EcR-B2 expression was observed in the developing MTs in embryos at stage 13 (Fig. 3X A and A′) and stage 15–16 (Fig. 3X C and C′).

Merged images showed the overlay of EcR-B2 and DAPI (Fig. 3X B, B′, D, D′) which confirmed EcR-B2 expression in MTs. Similarly EcR-B2 expression was observed in 1st (Fig. 3Y A and A′) and late 3rd instar larval MTs (Fig. 3Y C and C′). EcR-B2 expresses in both types of cells (PCs and SCs) of MTs. Merged images (Fig. 3Y C, C′ F and F′) showed the overlay of DAPI and EcR B2.

Cytoskeletal elements are disorganized upon ecdysone signaling disruption and is rescued by co-expression of ecdysone receptor isoforms

Epithelial morphogenesis is very much dependent on proper cytoskeletal organization, therefore the organization of cytoskeletal proteins was examined in the mutant MTs and compared to wild type. A characteristic pattern of β-tubulin was observed in the wild type with more expression in SCs (Fig. 4X A, white arrow) compared to PCs (Fig. 4X A, red arrow). Disruption of ecdysone signaling in *c42 > EcR-DN* larvae led to disrupted β-tubulin organization (Fig. 4X D) and the prominent tubulin expression in SCs was also reduced (Fig. 4X D, white arrow). On expressing the different isoforms with EcR-DN it was observed that expression of EcR-B2 (Fig. 4X M) and EcR-B1 (Fig. 4X J) restored β-tubulin organization similar to wild type (Fig. 4X A) but not in EcR-A (Fig. 4X G). The expression of β-tubulin was also restored similar to wild type in SCs of *c42 > EcR-DN;EcR-B1* (Fig. 4X J, white arrow) and *c42 > EcR-DN;EcR-B2* (Fig. 4X M, white arrow). The total intensity of β-tubulin expression in MT was measured by profile display function of LSM 510 Meta software and plotted on a graph (Fig. 4X P), which clearly supported the above results.

The organization of microfilaments was also observed by staining F-actin with phalloidin, which revealed that F-actin was arranged in bundles and organized in specific manner in MTs in wild type (Fig. 4Y A, white arrow). Similar to β-tubulin, F-actin bundles in the MTs of *c42 > EcR-DN* were disorganized (Fig. 4Y B, white arrow). This phenotype was reverted back near to wild type by EcR-B2 to maximum extent (Fig. 4Y E, white arrow) while EcR-A (Fig. 4Y C) and EcR-B1 (Fig. 4Y D) could not revert back F-actin organization in the MTs.

Disruption of ecdysone signaling in PCs up regulates the expression of (Na^+/K^+)-ATPase in MTs

Since ecdysone signaling affects the development of MTs, we were interested to look at the physiological functions of MTs. (Na^+/

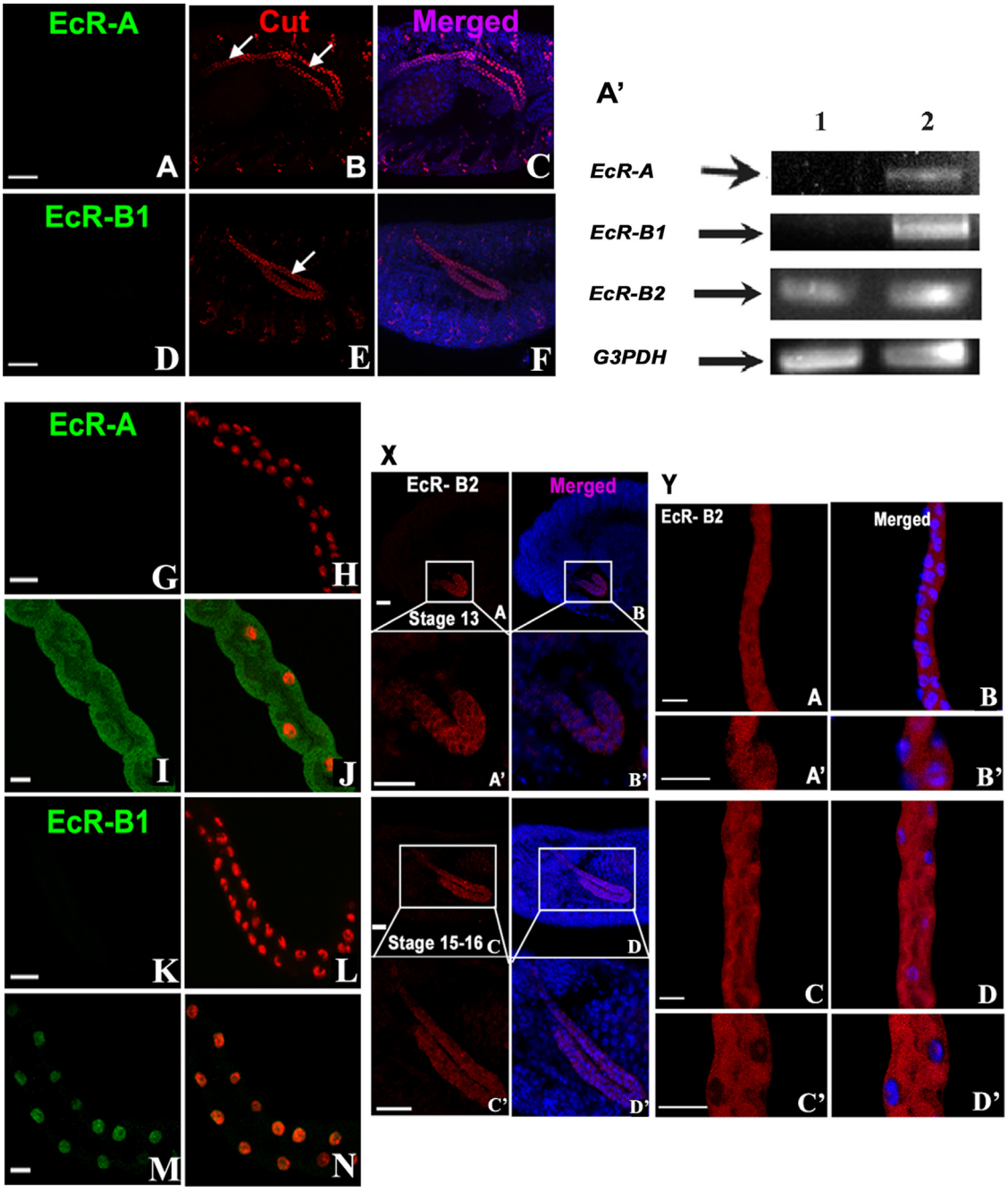

Fig. 3. Expression of EcR A, B1 and B2 in MTs. Absence of EcR-A (A) and B1 (D) signals in the MTs suggest that EcR-A and B1 do not express during embryonic development (stage 14-15). MTs were identified by anti-cut antibody (B, E). Merged images show the overlay of red (Cut) and blue (DAPI) (C, F) (Scale bar 20 μm). EcR-A and B1 do not express in the 1st instar larval MTs (G and K). In MTs of wandering larvae, EcR-A expression is nuclear as well as cytoplasmic (I), while EcR-B1 expresses only in nucleus (M). Merged images (H, J, L, N) show the overlay of green (EcR) and red (DAPI). (Scale bar 20 μm). [A′] RT-PCR analysis showed that only EcR-B2 expresses in the 1st instar, while all of them *EcR-A*, *B1* and *B2* express in wandering larvae. *G3PDH* was used as positive control. Lane 1 and 2 represents 1st and 3rd instar larval MTs respectively. [X] *Insitu* hybridization showed that EcR-B2 expresses in MTs at stage 13 and 15-16 (A and C) magnified view (A′ and C′). (Scale bar 20 μm). [Y] EcR-B2 expresses in the 1st (A, projection view) and 3rd instar larval MTs (C, projection view). Single section of 1st instar larval MT (A′) and 3rd instar larval MT (C′) shows that EcR-B2 is localized in cytoplasm and nucleolus. Merged images (B, B′, D, D′) shows the overlay of red (EcR-B2) and blue (DAPI). (Scale bar 20 μm in each case except in A′, B′, C′, D′ scale bar 10 μm).

K^+)-ATPase is a channel protein conserved from lower to higher organisms and plays a very important function in regulation of ionic balance in the cells (Roy et al., 2013). In adult and 3rd instar MTs, (Na^+/K^+)-ATPase has been reported to localize to the basolateral surface (Torrie et al., 2004; Verma and Tapadia, 2014), but due to absence of any report in 1st instar, we observed the expression of (Na^+/K^+)-ATPase in these larval MTs first. Results showed that similar to adults and 3rd instar larvae, (Na^+/K^+)-ATPase is expressed in the basolateral surface of the PCs as observed in the surface view (Fig. S4A) and mid saggital section (Fig. S4 B) of initial segment and in the main segment, surface view (Fig. S4 C), as well as mid-saggital section (Fig. S4 D). Na^+/K^+-ATPase does not express in the SCs (Fig. S4 A and E), identified by teashirt staining (Fig. S4 F). Nuclei were counterstained with DAPI (Fig. S4 G) and merged image (Fig. S4 H) showed the overlay of (Na^+/K^+)-ATPase, Teashirt and DAPI which confirms that (Na^+/K^+)-ATPase does not express in SCs. After disrupting ecdysone signaling in the PCs, an upregulation of (Na^+/K^+)-ATPase in *c42 > EcR-DN* (Fig. 5B) was observed when

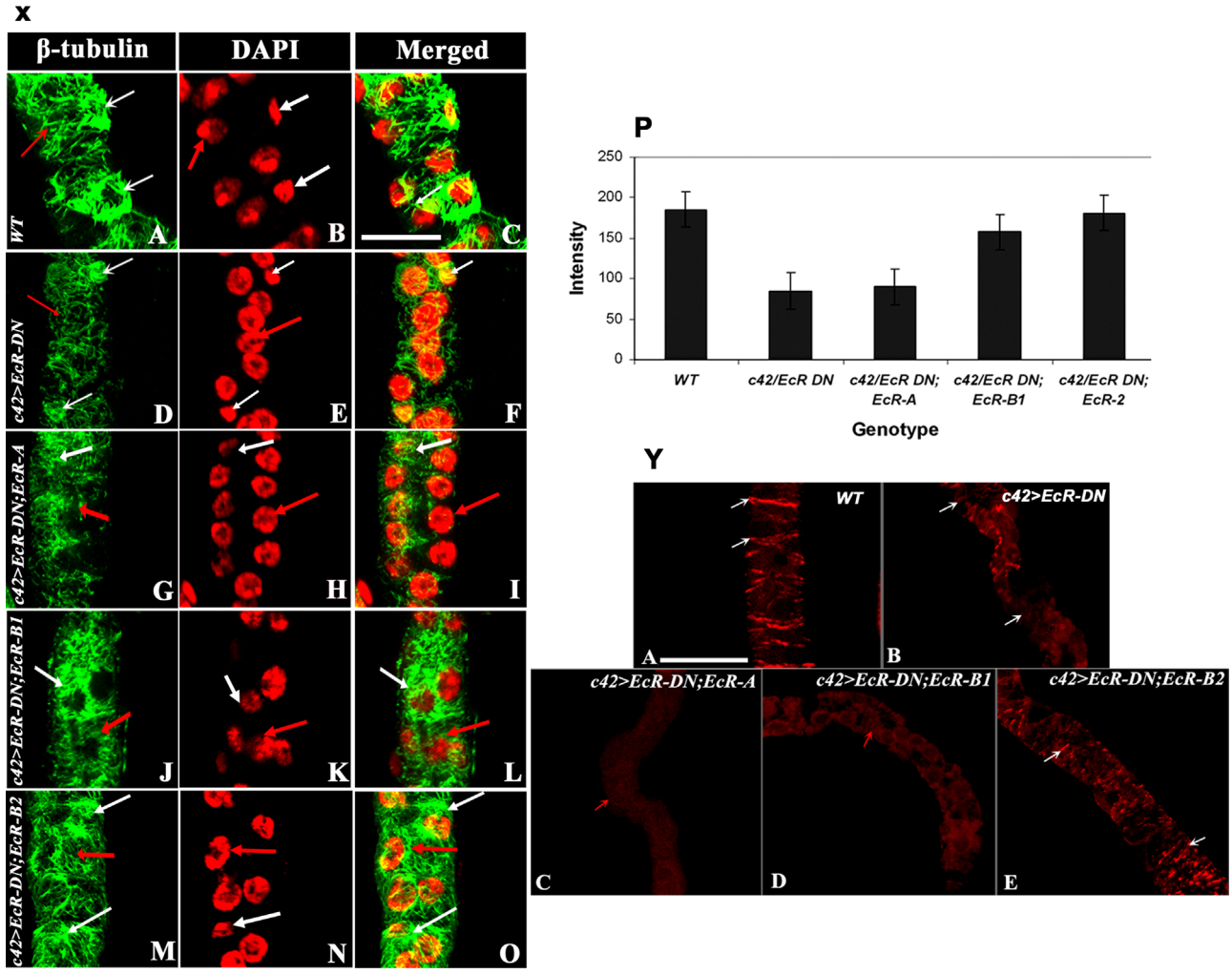

Fig. 4. Disruption of ecdysone signaling in the PCs affects the proper organization of β-tubulin and F-actin. [I] The organization of β-tubulin was disrupted in MTs of *c42 > EcR-DN* (D) in comparison to wild type (A). In wild type β-tubulin expresses abundantly in SCs (A, white arrows) compared to PCs (A, red arrow). Cells were identified by size of the nuclei as SCs have smaller nuclei (B white arrows) than PCs (B red arrow). Reduced expression of β-tubulin was observed in the SCs and in PCs (D, red arrow) of *c42 > EcR-DN* (D, white arrow). Co-expression of wild type EcR-B1 (J) and EcR-B2 (M) were able to rescue the β-tubulin organization almost same as wild type, while EcR-A did not. DAPI staining shows the chromatin in MTs (B, E, H, K, N). Merged (C, F, I, L, O) shows the overlay of β-tubulin and DAPI. (Scale bar 5 μm). Intensity of β-tubulin expression was measured by profile display function and plotted on graph (P) which confirms the above results. [II] The organization of F-actin was disrupted in MTs of *c42 > EcR-DN* (B, white arrow) compared to wild type (A, white arrow). Co-expression of EcR-B2 able to revert back F-actin organization to some extent (E, white arrow) while EcR-A (C, red arrow) and EcR-B1 (D, red arrow) were not able to do so (Scale bar 20 μm).

compared to wild type (Fig. 5A). This was confirmed by measuring the fluorescence intensity by profile display function of LSM 510 Meta software which showed upregulation of (Na^+/K^+)-ATPase expression in *c42 > EcR-DN* (Fig. 5b) in comparison to wild type (Fig. 5a). All images were captured at the confocal setting when –ve control shows basal peak of auto fluorescence (Fig. 5A0) in green channel.

To find out the ability of different isoforms to restore the expression of (Na^+/K^+)-ATPase, each isoform was co-expressed with EcR-DN. Maximum rescue was observed by co-expression of EcR-B2 (Fig. 5E) and then by EcR-B1 (Fig. 5D) isoforms, however, expression of EcR-A (Fig. 5C) had no effect on the levels of (Na^+/K^+)-ATPase and was same as in mutant. These results were confirmed by the line profile display function of LSM 510 Meta software which showed that the expression of (Na^+/K^+)-ATPase was restored in the MTs of *c42 > EcR-DN;EcR-B1* (Fig. 5d) and *c42 > EcR-DN;EcR-B2* (Fig. 5e) as wild type (Fig. 5a) whereas *c42 > EcR-DN;EcR-A* (Fig. 5c) was similar to *c42 > EcR-DN* (Fig. 5b). These results confirmed that co-expression of EcR-A was unable to restore EcR-DN induced elevated expression of (Na^+/K^+)-ATPase in the MTs. The results obtained by disrupting EcR-DN were validated using *ecd*^{1} mutant. The expression of (Na^+/K^+)-ATPase was elevated in *ecd*^{1} grown at 29 °C (Fig. 5B′ A) and comparable to *c42 > EcR-DN* (Fig. 5B′ D) whereas expression of (Na^+/K^+)-ATPase in *ecd*^{1} grown at 25 °C (Fig. 5B′ B) was similar to that of wild type (Fig. 5B′ A). These results suggested that ecdysone signaling is required for proper regulation of (Na^+/K^+)-ATPase in MTs. The intensity measurement by profile display function of LSM 510 Meta software clearly supported the above results.

To observe whether upregulation of (Na^+/K^+)-ATPase, after disruption of ecdysone signaling, also affected sodium ion concentration in the cells, we used sodium green fluorescent dye which fluoresces after binding to the free Na^+ ions (Minta and Tsien, 1989; George and Michael, 1995). There was an increase in fluorescence suggesting that there was an increase in free Na^+ concentration compared to wild type. These results were in agreements with earlier reports that reduced $(Na+/K+)$-ATPase resulted in reduced ion concentration (Davis et al, 1995; Verma and Tapadia, 2014). The mean fluorescence intensity was measured for 10 MTs in a constant area. The intensity in *c42 > EcR-DN* larval MTs (Fig. 6D) was 108.04 ± 21.5 (Fig. 6d) which was nearly 3 folds higher compared

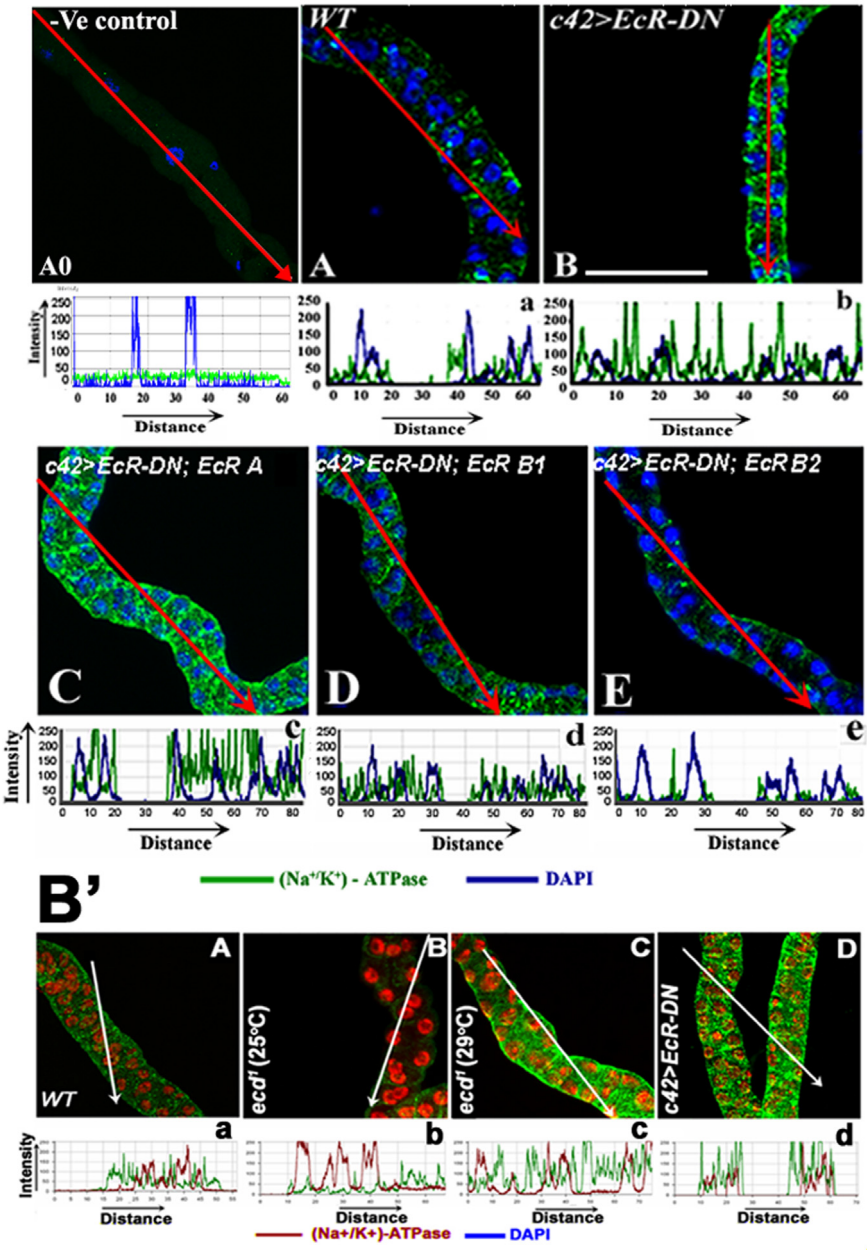

Fig. 5. Disruption of ecdysone signaling in MTs leads to up-regulation of (Na^+/K^+)-ATPase. [A′] Expression of EcR-DN in PCs leads to upregulation of (Na^+/K^+)-ATPase (B), compared to wild type (A). Co-expression of EcR isoform B1 and B2 was able to rescue (Na^+/K^+)-ATPase level in *c42 > EcR-DN;EcR-B1* (D) *c42 > EcR-DN;EcR-B2* (E) similar to wild type. Co-expression of EcR-A was not able to do so (C) and it remained as *c42 > EcR-DN* (B). A0 is negative control (Scale bar 20 μm). [B′] Ecdysoneless mutant, ecd^1 grown at 29 °C shows elevated expression of (Na^+/K^+)-ATPase (D) similar to *c42 > EcR-DN* in comparison to wild type (A). ecd^1 grown at 25 °C shows normal expression of (Na^+/K^+)-ATPase (B). Shown below each panel is the intensity of fluorescence as measured by Profile Display of LSM Meta 510 confocal microscope (A′a,b,c,d,e and B′a,b,c,d) (Scale bar 20 μm).

to wild type (Fig. 6A) which was 35.77 ± 18.2 (Fig. 6a). Co-expression of B2 isoform (Fig. 6G) was able to restore the Na^+ ion concentration 46.90 ± 13.7 (Fig. 6g) similar to wild type (Fig. 6a). Co-expression of EcR-B1 was also able to restore Na^+ concentration to certain levels, but not with EcR-A (data not shown). These results were confirmed using ecd^1 mutant where it was observed that net Na^+ concentration increased more than 3 folds (Fig. 6M and m) at 29 °C while the larvae grown at 25 °C (Fig. 6J, j) showed Na^+ concentration similar to wild type (Fig. 6A, a). Statistical analysis confirmed that Na^+ concentration in *c42 > EcR-DN* and ecd^1 at 29 °C was significantly more in comparison to wild type.

Further we wanted to know whether disruption of (Na^+/K^+)-ATPase directly affects Na^+ ion concentration in MTs, we checked Na^+ ion levels in (Na^+/K^+)-ATPase mutants (Palladino et al., 2003; Ashmore et al., 2009). Intensity of Na^+ was significantly reduced in mutants compared to wild type (Fig. 6B).

After observing that disruption of ecdysone signaling led to increased concentration of Na^+, it was presumed that this could also affect the concentration of other ions in the MTs like Cl^-, K^+ and Ca^+. To measure the levels of these ions, element detection system, EDS (energy dispersive X-ray spectrometer) of Zeiss scanning electron microscopy was used. It was observed that Na^+, Cl^-, K^+, and Ca^{++} ion concentration in MTs of *c42 > EcR-DN* was 44.8 ± 12.1, 3.7 ± 1.5, 49.1 ± 11 and 2.4 ± 1 respectively (Table 4). Similar results were obtained in ecd^1 grown at 29 °C where Na^+, Cl^-, K^+ and Ca^{++} ion concentration was 45.7 ± 13.8, 1.8 ± 0.9, 49.8 ± 14.3 and 2.7 ± 1.4 respectively (Table 4). In the wild type, Na^+, K^+, Cl^- and Ca^{++} ion concentration in MTs was

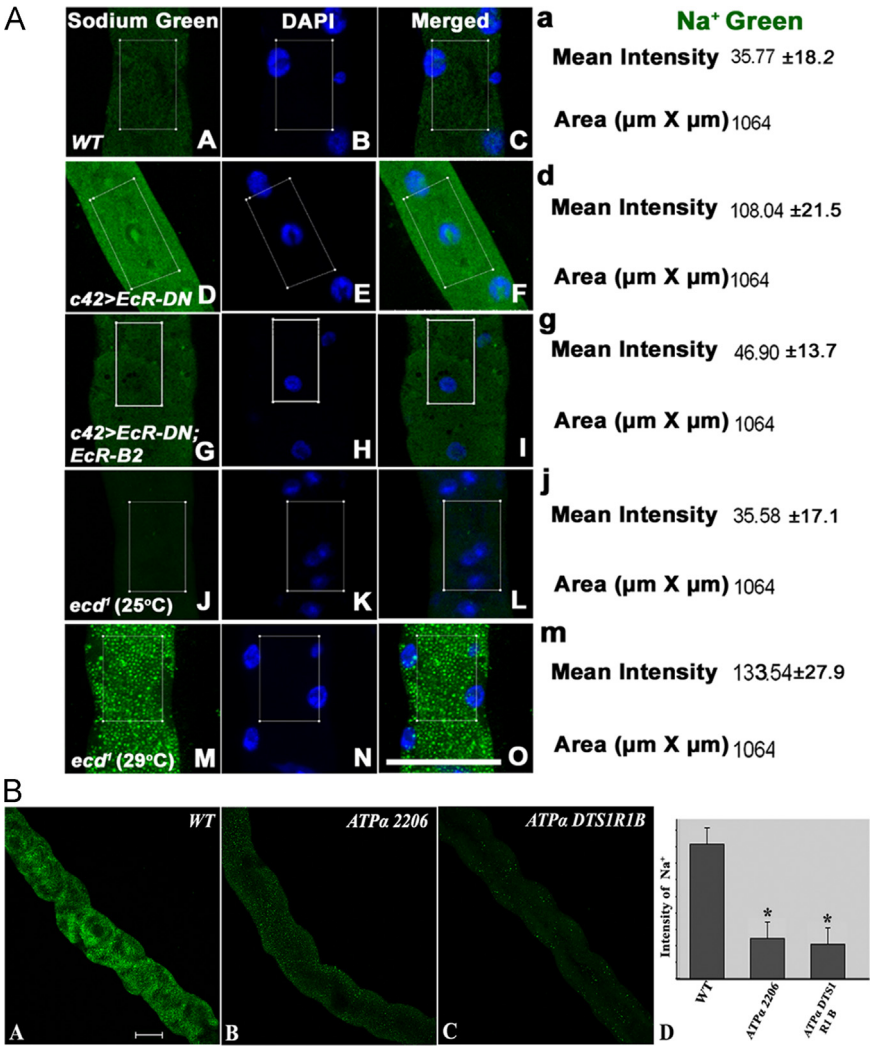

Fig. 6. [A] Disruption of edysone signaling in MTs upregulates the Na^+ ion concentration in the MTs. Sodium Green is the cell permeable dye, which fluoresces after binding to free Na^+ ions in cells. Disruption of ecdysone signaling in the *c42 > EcR-DN* (D) increases the mean intensity by 3 folds when compared to wild type (A). In *c42 > EcR-DN; EcR-B2* (G) fluorescence was similar to wild type (A). Similarly in *ecd*^{1} grown at 29 °C (M) the concentration of Na^+ increased compared to *ecd*^{1} grown at 25 °C (J). (Scale bar 5µm). The area (1064 μm^2) used to measure the intensity was constant in each case. Graph showing the total fluorescence from 1 unit area (a,d,g,j,m). [B] Reduced concentration of Na^+ ion in MTs of Na^+/K^+ ATPase mutant larvae: Na^+ concentration was reduced in the MTs of ATPα 22006 (B) and ATPα DTS1 R1B (C) compared to WT (A). Statistical analysis suggest that differences in Na^+ concentration is significant (D) ($P > 0.05$).

Table 4
Disruption of ecdysone signaling in MTs disrupt the ionic balance in the tissue. Increase Na^+ and K^+ ion concentration in the MTs of ecdysoneless *ecd*^{1} mutant grown at 29 °C (B) and *c42 > EcR-DN* (C) compare to wild type (A) while Ca^{2+} and Cl^- ion concentration decreases. In the *c42 > EcR-DN; EcR-B2* (D) the ion concentration were similar to wild type (A). The values given for the ions are the relative percentage value measured by electron dispersive system of Zeiss scanning electron microscope and do not represent the exact concentrations of ions in the cells. *N* shows total number of tubule taken for sample preparation in each case.

Genotype ($N=5$)	Na^+	Cl^-	K^+	Ca^{++}
+/+	15.4 ± 11.7	18 ± 9.2	28 ± 13.5	38.5 ± 12.4
ecd^1 (29 °C)	45.7 ± 13.8*	1.8 ± 0.9*	49.8 ± 14.3*	2.7 ± 1.4*
c42 > EcR-DN	44.8 ± 12.1*	3.7 ± 1.5*	49.1 ± 11.5*	2.4 ± 1.1*
c42 > EcR-DN;EcRB2	17.2 ± 12.1	13.7 ± 10.3*	29.6 ± 11.5	39.2 ± 14.8

* Mean difference is significant at the level of 0.05. Dunnett's *t*-test was performed with wild type as a control.

15.4 ± 11.7, 18.0 ± 9.2, 28.0 ± 13.5 and 38.5 ± 12.4 respectively (Table 4). Statistical analysis showed that there were significant differences in ion concentration in mutant compared to WT (Table 4). Co-expression of EcR-B2 restored the ion concentration in the MTs similar to wild type (Table 4). The concentration of Na^+, K^+, Cl^- and Ca^{++} ion in *ecd*^{1} mutant grown at 25 °C was also similar to that of wild type (data not shown). The values given for the ions are the relative percentage value measured by electron dispersive system of Zeiss scanning electron microscope and do not represent the exact concentrations of ions in the cells.

Disruption of ecdysone signaling in MTs affects uric acid deposition

Uric acid is an excretory product that is deposited in the lumen of MTs (Wigglesworth, 1965; Bursell, 1967). The crystals of uric acid are clearly visible in the birefringence light (Allan et al., 2005; Hirata et al., 2012). So, in the light of disruption of channel proteins in PCs, we studied the function of MTs by observing uric acid deposition. A reduction in the deposition of uric acid in the MTs was observed when ecdysone signaling was disrupted in PCs (Fig. 7X B′).

These results were also validated using *ecd*^{1} grown at 29 °C which showed reduced uric acid deposition (Fig. 7Y D′) compared to wild type (Fig. 7Y A′). The larvae of *ecd*^{1} grown at 25 °C (Fig. 7Y C′) and larvae of wild type (Fig. 7Y B′) grown at 29 °C were used as

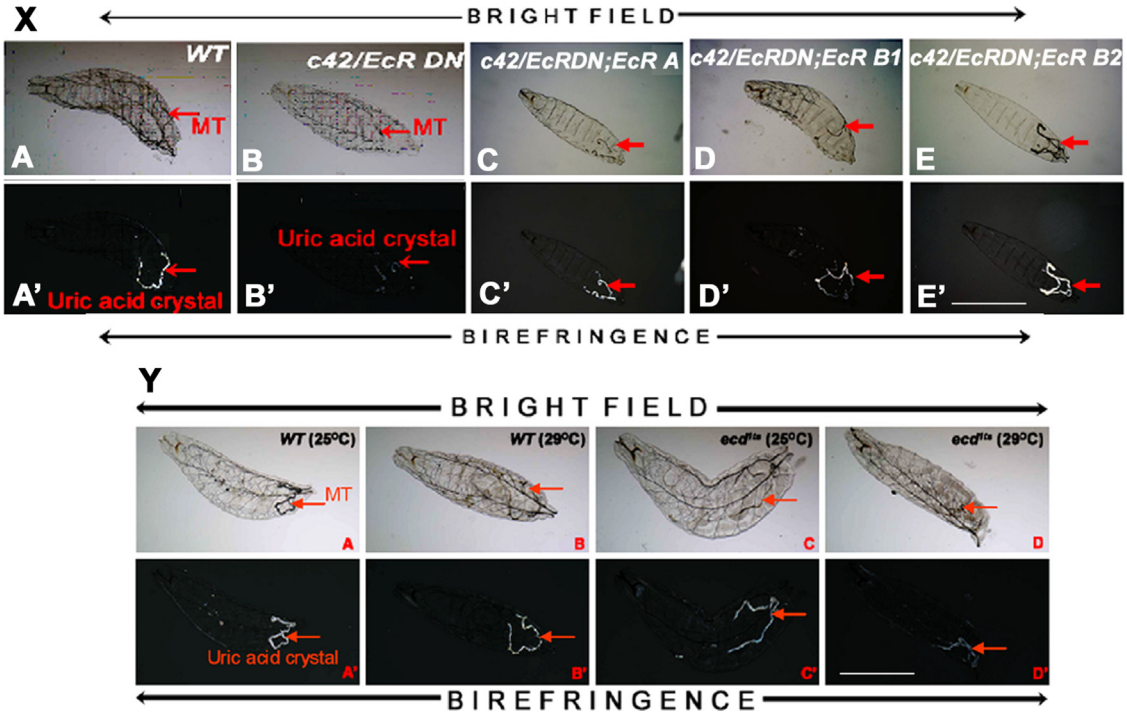

Fig. 7. Disruption of ecdysone signaling in MTs reduced uric acid deposition [X] Disruption of ecdysone signaling in principal cells reduces the deposition of uric acid in the MTs (B′) compared to wild type (A′). Co-expression of EcR-A, B1 and B2 with EcR-DN could restore the uric acid deposition as observed in *c42 > EcR-DN; EcR-A* (C′), *c42 > EcR-DN; EcR-B1* (D′), *c42 > EcR DN;EcR-B2* larvae (E′). Corresponding images of wild type (A), *c42 > EcR-DN* (B), *c42 > EcR-DN; EcR-A* (C), *c42 > EcR-DN; EcR-B1* (D), *c42 > EcR DN; EcR-B2* (E) larvae (C) were captured in the bright field (Scale bars represent 100 μm). [Y] Disruption of ecdysone signaling in the MTs in ecd^1 at 29 °C causes reduced level of uric acid deposition (D′) compared to wild type (A′). Larvae of ecd^1 grown at 25 °C (C′) and wild type (B′) grown at 29 °C (C′) showed uric acid deposition similar to wild type grown at 25 °C. Corresponding images of larvae of *WT* at 25 °C (A), *WT* at 29 °C (B) ecd^1 at 25 °C (C), ecd^1 grown at 29 °C (D) were captured in the bright field (Scale bars represent 100 μm).

controls and uric acid deposition was similar to wild type grown at 25 °C. The larvae were also observed in bright field to confirm the presence of crystals in MTs (Fig. 7X A, B, C and D and Fig. 7Y A, B, C and D). Above results clearly showed that disruption of ecdysone signaling in the PCs altered the functional properties of tubules resulting in reduced deposition of uric acid. In order to find out which isoform of EcR was able to restore these phenotypes, the different isoforms A, B1 and B2 of EcR were co-expressed and restoration was observed with EcR-A (Fig. 7X C′), B1(Fig. 7X D′) and B2 (Fig. 7X E′) to different extents. Restoration with EcR-B2 was maximum compared to wild type, followed by B1 and A.

Discussion

Drosophila MTs prove to be a good model to understand development for three reasons, first, they are made up of cells originating from ectoderm and mesoderm which intercalate in a regular manner to form functional tubules (Denholm et al., 2003; Jung et al., 2005; Singh et al., 2007; Gautam and Tapadia, 2010; Tapadia and Gautam, 2011) second, these cells of different origins have physiologically distinct functions (Dow et al., 1994; O'Donnell et al., 1996; Davies et al., 1996; Sozen et al., 1997; O'Donell et al., 1998; Denholm et al., 2003; Verma and Tapadia, 2012) and third, they do not undergo ecdysone induced degeneration during metamorphosis (Jiang et al., 1997; Gautam and Tapadia, 2010; Tapadia and Gautam, 2011).

The present study shows a new role of ecdysone in the development of MTs, affecting the distribution and number of SCs and PCs in MTs. The primordium specification by genes like *tailless* (*tll*), *huckebein* (*hkb*), *fork head* (*fkh*) and *Wingless* (*wg*) (Janning et al., 1986; Weigel et al., 1989; Skaer, 1989; Harbecke and Janning, 1989; Gaul and Weigel, 1990; Smith and Orr-Weaver, 1991; Skaer, 1993; Harbeck and Langyel, 1995; Wu and Langyel, 1998) does not appear to be affected after disrupting ecdysone signaling as MTs do develop, however the MTs are reduced in size, suggesting that genes involved in proliferation are probably affected. We show that expressing EcR-DN in PCs leads to reduction in the number of both, PCs and SCs, which could be responsible for the reduction in size of the tubules. This is in contrast to our earlier results where we have shown that expressing EcR-DN in SCs affects the number of SCs only and not the PCs (Gautam and Tapadia, 2010), suggesting that disruption of ecdysone signaling in the PCs has more global effect than that in SCs. Proliferation of cells in MTs is under the influence of epidermal growth factor receptor (EGFR) signals emanated from the single tip cell which is received by the distal neighboring cells resulting in cell division. One of the regulators of cell proliferation is *seven-up* (*svp*) which encodes a homolog of human transcription factor COUP-TF (Mlodzik et al., 1990; Power et al., 1991) and belongs to steroid/thyroid hormone receptor superfamily (Thummel, 1995). It has been postulated that *svp* can heterodimerize with subunits of ecdysone receptor and regulate gene expression (Power et al., 1991; Zelhof et al., 1995). From the present results it is possible to believe that *svp* can be a potent candidate to be regulated by ecdysone signaling. The second possibility that ecdysone regulates EGFR signaling in MTs development cannot be ruled out at the moment. The MTs cell number does not seem to be reduced in *rolling pebbles* (*rols*) mutants (Putz et al., 2005) but is reduced after disrupting ecdysone signaling, suggesting that ecdysone acts early in the development of MTs. The reduction in SCs number could be a consequence of ecdysone regulating factors that might be involved in mesodermal cell division or might be preventing intercalation in the MTs.

Apart from the reduced cell numbers, a second manifestation is that the regular pattern of PCs and SCs are disrupted. The arrangement of PCs is controlled largely by the product of *rols*, since in *rols* mutants, while PCs were in clusters, the SCs integrated normally (Putz et al., 2005). The *rols* mutants have defects in the passage of

tubules through the body cavity and loss of rearrangement of cells, which, results in more than two PCs surrounding the MTs lumen than the characteristic two cells as observed in wild type. Since the expression of *rols* is from stage 15 onwards, the arrangement of SCs was not affected (Putz et al., 2005), as by this time the SCs would have incorporated in the tubules (Denholm et al., 2003). In the present study we suggest that ecdysone signaling affects in PCs before the SCs intercalation. Since, ecdysone deficiency leads to clustering of PCs, so the proper intercalation of SCs is consequently affected. Thus the aberrant distribution and reduced number of SCs are consequence of PCs clustering due to ecdysone deficiency.

Ecdysone transduces its signal through three isoforms, EcR-A, EcR-B1 and EcR-B2. The role of EcR-A and EcR-B1 (Schubiger et al., 1998; Cherbas et al., 2003; Davies et al., 2005) has been well documented but the role of EcR-B2 has not been studied because of lack of specific mutants and absence of specific antibodies. Through the present study we show that EcR-B2 isoform is the major isoform in the MTs through which ecdysone signaling is transduced. However the requirement of the EcR isoform for the two cell types is slightly different as SCs exclusively uses EcR-B2 isoform (Gautam and Tapadia, 2010) whereas PCs shows some redundancy as observed in the present results. It primarily responds to EcR-B2, but in the absence of EcR-B2, EcR-B1 can take over the functioning, though to lesser extent than EcR-B2. EcR-A is also able to rescue but not to the same extent as EcR-B1

It is notable in this context that migration of border cells in egg chambers requires C/EPB transcription factor encoded by *slow border cells* (*slbo)* locus and in *slbo* mutants, border cells migrate either very slowly or not at all (Cherbas et al., 2003). Expression of EcR-DN driven by *slbo-Gal4* in ovaries, results in failure of border cells migration, which is subsequently rescued by the expression of EcR-B2 isoform (Cherbas et al., 2003). In view of the present results, it is tempting to speculate that migration of cells to achieve different developmental fates is triggered by ecdysone and EcR-B2 is the key isoform that transduces the signal. This also strengthens the observation that migratory cells require EcR-B2 isoform as observed for border cells (Cherbas et al., 2003) and SCs (Gautam and Tapadia, 2010).

Tubule elongation depends on cell rearrangements following proliferation, and requires other factors like cell migration and cell–cell recognition and adhesion which are governed by cytoskeletal and cell junctional proteins. Members of Rho-GTPase family have been shown to modulate cytoskeleton elements (Hall, 1998). In the present paper we show that ecdysone signaling could also be one of the factors for misorganization of cells in MTs as microfilaments and microtubules are disrupted. *Myoblast city* (*mbc*) mutant embryos exhibit a strong muscle fusion phenotype and Mbc is involved in dorsal closure and cytoskeletal organization (Doberstein et al., 1997; Erickson, et al., 1997). *mbc* mutants display defects in tubule organization, in which anterior MTs are displaced and misguided within embryo (Ainsworth et al., 2000). Mbc, the homolog of vertebrate DOCK180 in *Drosophila*, associates with the adapter protein Crk (Erickson et al., 1997; Nolan et al., 1998; Galletta et al., 1999), which regulates cell migration and cytoskeleton organization in a Rac-dependent manner (Hasegawa et al. 1996; Kiyokawa et al., 1998; Gade et al., 1997; O'Donnell and Spring, 2000). It is possible that Mbc is also disrupted in the present study and is regulated by ecdysone. However, it cannot be said whether disruption of cytoskeleton is the cause or effect of malformed tubules.

Fluid homeostasis and removal of toxic substances is critical to life of an organism and these functions are carried out by specialized organs like kidneys in human and MTs in *Drosophila*. There are several specific set of transporters which very efficiently reduce the toxic burden of organisms and maintain osmotic balance. (Na^+/K^+)-ATPase, an electrogenic pump is responsible for maintaining the balance of Na^+ and K^+ in almost all animal cells. Na^+/K^+-ATPase is critical to a variety of physiological processes like osmoregulation, cell volume regulation, transport of certain amino acid and sugar and maintenance of membrane excitability (Ianowski and O'Donnell, 2004, Verma and Tapadia, 2014, Roy et al., 2013). Direct correlation of Na^+/K^+-ATPase levels and Na^+ concentration was rather surprising in the present study, but it is in agreement with earlier reports where reduced levels of (Na^+/K^+)-ATPase resulted in reduced Na^+ (Davis et al, 1995; Verma and Tapadia, 2014). Similar results with (Na^+/K^+)-ATPase mutants suggested that in MTs, (Na^+/K^+)-ATPase function differently as compared to the general assumption (3 Na^+ exported per 2K^+ imported) (Schooley et al., 2012). The altered (Na^+/K^+)-ATPase levels also differentially impacted the levels of different ions like Na^+, K^+, Ca^{++} and Cl^- ions. There are several factors like, serotonin activity, Na^+/H^+ exchanger activity and hemolymph K^+ and Na^+ levels which might affect the Na^+ ion concentration.

The overall effect of disruption of ecdysone signaling in MTs finally results in lethality, which appears surprising as to how malformed tubules lead to lethality. Earlier studies have shown that expression of *EcR-DN* with *Eip*, *GMR*, *Ser* or *dpp* Gal4 drivers revealed local as well as a global effects resulting in complete blockage of development (Cherbas et al., 2003), suggesting that prior to every molting there is a checkpoint which signals the organism to proceed further for development. It is likely that localized malfunctioning of EcR in important tissues is sensed by the surveillance system and in case of irreparable damage, development is halted at the next ecdysone dependent event. The data strongly suggests that proper development of MTs could also be one of the critical tissues for the survival of the organism whose malformation ultimately leads to larval death.

In *Drosophila* the integration of mesenchymal cells with the developing epithelial tubule is required for the physiological maturation of MTs (Denholm et al., 2003). Parallel to this in vertebrates, the recruitment of mesenchymal cells to epithelial tissues underpins the development of vertebrate kidney. Failure in the process of recruitment of mesenchymal cells to epithelial cells leads to polycystic kidney and in severest cases, to renal agenesis (Khoshnoodi and Tryggvason 2001). What is important is that there has to be a perfect coordination between these two functions, because disturbing the function in any one cell types causes a global phenotype leading to lethality. In the present study we have unequivocally shown that ecdysone regulates the organization of MTs and also controls ionic balance by regulating (Na^+/K^+)-ATPase, however, the other players in between ecdysone and these functions is still to be understood. We also show a novel function for EcR-B2 in the development and function of MTs.

Materials and methods

Fly stocks and rearing condition

The fly stocks used for the study were obtained from Bloomington stock centre except where mentioned. *Oregon* R^+ was used as a wild type control. Gal4 driver *c42,* (gift from Dr. J.A.T. Dow, University of Glassgow, Glasgow). The expression domains of *c42* were studied using UAS-GFP results shown in Fig. S1. EcR dominant negative UAS responders, *P{UAS-EcR.B1-DeltaC655.F645A},* wild type EcR isoforms UAS responder, *P{UAS-EcR.B1}, P{UAS-EcR.B2} P{UAS-EcR.A}.* Appropriate crosses were setup to generate *P{UAS-EcR.B1-ΔC655.F645A}; P{UAS-EcR.B1}, P{UAS-EcR.B1-DeltaC655.F645A}; P{UAS-EcR.B2}, P{UAS-EcR.B1-DeltaC655.F645A}; P{UAS-EcR.A}, P{UAS-EcR.B1-DeltaC655.W650A}; P{UAS-EcR.B1}, P{UAS-EcR.B1-DeltaC655.W650A; P{UAS-EcR.B2}, P{UAS-EcR.B1-DeltaC655.W650A; P{UAS-EcR.A}}.* Temperature sensitive hypomorph allele of ecdysone, *ecd*^{1} *st*^{1} *red*^{1} *e*^{4} *ca*^{1} (Garen et al., 1977, kind gift from Dr. C. Thummel, University of Utah, Salt

Lake City, UT). *ecd*^{1} flies were allowed to lay eggs at 29 °C and allowed to develop till they were dissected for study.

Na^+/K^+-ATPase mutants, *W–; ATPα DTS1R1B/TM3*, *Sb,Ser* and *ATPα 2206* (kind gift from Dr. Palladino, University of Pittsburg, PA). All flies were reared at 25 ± 1 °C on standard food containing maize powder, agar, dried yeast and sugar.

Viability assays

Flies of different genotypes were allowed to lay eggs on agar plates. Eggs were counted and left for further development. The hatched larvae were transferred on the food plates and lethality was scored at each stage. The number of eclosed adults was finally used to measure the percentage viability.

Cuticular preparation of larvae

Dying/dead larvae of desired genotypes were fixed in glycerol and acetic acid in 1:4 ratio and kept at 60 °C overnight. Fixed larvae were mounted on clean glass slide in Hoyer's mountant and kept at 60 °C overnight. Bright field images were captured using Nikon Digital camera DXM 1200 fitted on the Nikon E800 microscope.

Dechorionation and devitellinization of embryos

Embryos of desired genotypes were dechorionated in 50% sodium hypochlorite for 3 min and washed with distilled water for 2 min followed by heptane for 1 min. These embryos were fixed with paraformaldehyde (4%) and heptane solution for 20–30 min. Fixative was removed and embryos were washed twice with heptane. These embryos were devitellinized with heptane and methanol solution. Devitellinized embryos were washed 2–3 times in methanol. Next, the embryos were rehydrated through down graded methanol (90%, 70%, 50%, 30%, 10%,) with PBT (1X PBS pH 7.4, 0.5% Triton-X-100) 5 min each, again washed with 1X PBS thrice for 5 min each. Further these embryos were used for immunostaining and in-situ hybridization.

Immunostaining

MTs of desired genotypes were dissected from dying/dead larvae in 1X Phosphate buffer saline (PBS), fixed in 4% paraformaldehyde for 20 min at RT, washed in PBT thrice for 15 min, blocked in the blocking solution for 2 h at RT followed by overnight incubation in primary antibodies at 4 °C. The tissues were washed in PBT thrice for 15 min each and incubated with secondary antibody for 2 h at RT. Tissues were again washed thrice in PBT, followed by counter staining in DAPI (1 μg/ml) for 15 min at RT. Tissues were washed again in PBT at RT three times and mounted in antifadent DABCO (1,4 diazobicyclo acetone) and observed under confocal microscope.

Expression domain of Gal4 driver

The Gal4 driver c42 was crossed with UAS-GFP to observe its expression domains in development. The expression patterns of green fluorescence protein (GFP) in embryonic and larval stages suggest that the Gal4 driver *c42* expresses in the principal cells of MTs (Fig. S1). In 1st instar larval MTs expression is limited to the PCs (Fig. S1, C, C′, C″) however at 3rd instar larval stage, expression was also observed in bar type SCs of initial segment along with PCs (data not shown) as reported earlier by Rosay et.al. in 1997. GFP expression pattern also suggested that *c42* has leaky expression in salivary glands.

Reverse transcriptase polymerase chain reaction (RT-PCR)

For semiquantitative RT-PCR analysis, total RNA was isolated from the MTs of the desired genotypes using TRIZOL reagent following the manufacturer's recommended protocol (Sigma-Aldrich, India). cDNA was synthesized from total RNA using 200U of M-MuLV reverse transcriptase (New England Biolabs, USA) One-tenth volume of the reaction mixture was subjected to PCR using specific primers. Specific primers for N-terminal domain of EcR-A, EcR-B1 and EcR-B2 were used (Bioserve, Hyderabad, India). GPDH was used as internal control. Thermal cycling parameter for EcR A and B1 were 95 °C (2 min), 27 cycle of {95 °C (30 s), 50 °C (45 s), 72 °C (2 min)} 72 °C for 4 min. PCR condition for EcR-B2 was same as described for EcR-A and B1 only final extension time was 8 min due to large fragment size.

Preparation of DIG-labeled DNA probe

Digoxygenin labeled probes were prepared by random priming (Feinberg and Vogelstein, 1983) using the non-radioactive DIG-DNA labeling kit (Roche, Germany). 2–2.5 μg of the linearized DNA fragment of EcR-B2 was taken in a microfuge tube and the volume was made up to 15 μl with distilled water. DNA was denatured by heating in a boiling water bath for 10 min, followed by quick chilling on ice. 2 μl (10 ×) of random hexanucleotide primer mix, 2 μl of dNTP mix (0.1 mM each of dATP, dGTP and dCTP; 0.065 mM of dTTP and 0.035 mM of DIG-dUTP) and 2 μl of the Klenow enzyme (2U) was added and the reaction mixture was incubated at 37 °C for 16 h. The reaction was stopped by adding 2 μl of 0.2 M EDTA (pH=8). The labeled DNA was precipitated by adding 2 μl of Salmon sperm DNA (10 mg/ml), 2.5 μl of 4M $LiCl_2$ and 75 μl of pre-chilled absolute ethanol. After centrifugation, the pellet was dried and dissolved in TE at a concentration of 25 ng/μl. The labeled DNA was stored at −20 °C.

DNA-RNA in situ hybridization

Larval MTs and dechorionated and devitellinized embryo were collected and fixed with 4% PFA. Re-fixation was done with 4% PFA and 0.6% Triton-X in 1 × PBS at RT for 20 min and washed in PBT (1 × PBS, 0.1% Triton-X) 5X5 min. After washing, digested with proteinase K (10 μg/ml) for 4 min at RT and washed with chilled PBT and glycine solution (2 mg/ml) for 2 × 5 min. Again fixed in 4%PFA, 0.2% gluteraldehyde in 1 × PBS for 15 min and washed 5 × 5 min in PBT. Tissues were incubated in 1:1 mixture of PBT: Hybridization buffer (50 % formamide, 5 × SSC, 10 μg/ml yeast-*t*-RNA, 100 μg/ml salmon sperm DNA, 50 μg/ml Heparin, 0.1% Tween-20 in DEPEC water) for 10 min at RT, followed by 1 h at 48 °C in hybridization chamber. Heat denatured DIG labeled probe diluted in hybridization buffer was added and kept at 48 °C in hybridization chamber for 36 h. After hybridization, samples were washed in hybridization buffer at 48 °C for 30 min. Then washed in hybridization buffer and PBT in 1:1 ratio at 48 °C in hybridization chamber for 30 min. Washed in hybridization buffer and PBT in 1:2 for 10 min. Washed in PBT 2X5′. Blocked in blocking solution for 2 h at RT. Incubated in anti-DIG rhodamine at dilution 1:200 at RT. Wash in PBT for 15 × 5 min. Counterstained with DAPI and mounted in DABCO.

Measurement of ions concentration in MTs

Whole MTs were dissected out in 1X PBS and incubated in cell permeable fluorescent dye Na^+ green (Molecular Probes) which binds to free Na^+ ions. Na^+ ion concentration was measured using profile display function of Zeiss LSM 510 Meta confocal microscope (Verma and Tapadia, 2014).

Na^+ concentration was reconfirmed by element detection system. Five pairs of dissected tubules were kept in a drop of 5 μl of 1X PBS for 30 min in moist chamber at room temperature. After 30 min tubules were removed, PBS was allowed to dry and then sample prepared for scanning electron microscopy (SEM) by the standard protocol (Goldstein, et al. 2003). After sample preparation, ions were measured by element detection system, (EDS, energy dispersive X-ray spectrometer) of Zeiss Scanning Electron Microscope (Verma and Tapadia, 2014)

Microscopy and documentation

Imunofluorescence stained preparation were observed under Nikon E800 fluorescence microscope using appropriate filter or under Zeiss LSM 510 Meta laser scanning confocal microscope. The images on the Nikon E800 microscope were recorded with Nikon digital camera DXN 1200. All the images were processed and assembled using Adobe Photoshop 7.0. *Drosophila* larvae and flies were viewed under Zeiss Stemi SV6 Stereo-binocular microscope and were photographed at a magnification upto 5× and digital zoom 6× using a sony digital camera (DSC-S75) fitted on microscope.

Statistical analysis

The data were tested for their significance using one way ANOVA followed by Dunnett's *t*-test for comparisons between more than two groups at 0.05 level significance. Dunnett's *t*-tests treat one group as a control, and compare all other groups against it.

Author contributions

Conceived and designed the experiments: NKG and MGT. Performed the experiments: NKG and PV. Analyzed the data: NKG, PV and MGT. Contributed reagents/ materials/analysis tools: NKG and MGT. Wrote the paper: NKG and MGT.

Acknowledgments

We are thankful to Dr. J. A. T. Dow, and Dr. C. Thummel for fly stocks and for their useful suggestions. We also thank Dr. S. Cohen, University of Copenhagen, Denmark for kindly providing anti-teashirt antibodies. We are very thankful to Prof S.C. Lakhotia, BHU for his critical comments and valuable inputs in the paper. We are thankful to Drs. R.S. Srivastava and G.C. Gautam, Department of Geology, BHU for polarized light microscopy. Dr. Monisha Banerjee is acknowledge for giving freedom to work at BHU for the present paper. We are thankful to Department of Science and Technology, Government of India, New Delhi for financial support to MGT and also for the Multiphoton Confocal Microscope National Facility. Financial support to NKG from ICMR, New Deilhi is greatly acknowledged.

Appendix A. Supporting information

Supplementary data associated with this article can be found in the online version at http://dx.doi.org/10.1016/j.ydbio.2014.11.003.

References

Ainsworth, C., Wan, S., Skaer, H., 2000. Coordinating cell fate and morphogenesis in *Drosophila* renal tubules. Philos. Trans. R. Soc. Lond. B Biol. Sci. 355, 931–937.
Allan, A.K., Du, J., Davies, S.A., Dow, J.A.T., 2005. Genome-wide survey of V-ATPase genes in Drosophila reveals a conserved renal phenotype for lethal alleles. Physiol. Genom. 22, 28–138.
Ashmore, L.J., Hrizo, S.L., Paul, S.M., Voorhies, W.A.V., Beitel, G.J., Palladino, M.J., 2009. Novel mutations a Vecting the Na^+/K^+-ATPase alpha model complex neurological diseases and implicate the sodium pump in increased longevity. Hum. Genet. 126, 431–447.
Bender, M., Imam, F.B., Talbot, W.S., Ganetzky, B., Hogness, D.S., 1997. *Drosophila* ecdysone receptor mutations reveal functional differences among receptor isoforms. Cell 91, 777–788.
Bursell, E., 1967. Excretion of nitrogen in insects. Adv. Insect Physiol. 4, 33–67.
Cherbas, L., Hu, X., Zhimulev, I., Belyaeva, E., Cherbas, P., 2003. EcR isoforms in *Drosophila*: testing tissue-specific requirements by targeted blockade and rescue. Development 130, 271–284.
Davies, M.B., Carney, G.E., Robertson, A.E., Bender, M., 2005. Phenotypic analysis of EcR A mutants suggests that EcR isoforms have unique functions during *Drosophila* development. Dev. Biol. 282, 385–396.
Davis, M.W., Somerville, D., Raymond, Y.N., Lee, R.Y.N., Lockery, S., Avery, L., Fambrough, D.M., 1995. Mutations in the Caenorhabditis elegans Na,K-ATPase a-Subunit Gene, eat-6, disrupt excitable cell function. J. Neurosci. 15, 8408–8418.
Davies, S.A., Goodwin, S.F., Kelly, D.C., Wang, Z., Sozen, M.A., 1996. Analysis and Inactivation of vha55, the gene encoding the Vacuolar ATPase B- subunit in *Drosophila melanogaster*, reveals a larval lethal phenotype. J. Biol. Chem. 271, 30677–30684.
Denholm, B., Sudarsan, V., Pasalodos-Sanchez, S., Artero, R., Lawrence, P., 2003. Dual origin of the renal tubules in *Drosophila*: mesodermal cells integrate and polarize to establish secretory function. Curr. Biol. 13, 1052–1057.
Doberstein, S.K., Fetter, R.D., Mehta, A.Y., Goodman, C.S., 1997. Genetic analysis of myoblast fusion: blown fuse is required for progression beyond the prefusion complex. J. Cell Biol. 136, 1249–1261.
Dow, J.A.T., Davies, S.A., Sozen, M.A., 1998. Fluid secretion by the *Drosophila* Malpighian tubule. Am. Zool. 38, 450–460.
Dow, J.A.T., Maddrell, S.H.P., Davies, S.A., Skaer, N.J.V., Kaiser, K., 1994. A novel role for the nitric oxide-cGMP signaling pathway: the control of epithelial function in *Drosophila*. Am J Physiol. 266, 1716–1719.
Erickson, M.R., Galletta, B.J., Abmayr, S.M., 1997. *Drosophila* myoblast city encodes a conserved protein that is essential for myoblast fusion, dorsal closure, and cytoskeletal organization. J. Cell Biol. 138, 589–603.
Feinberg, A.P., Vogelstein, B., 1983. A technique for radiolabeling DNA restriction endonuclease fragments to high specific activity. Anal. Biochem. 132 (1), 6–13.
Gade, G., Hoffmann, K.H., Spring, J.H., 1997. Hormonal regulation in insects: facts, gaps and future directions. Physiol. Rev. 77, 963–1032.
Galletta, B.J., Niu, X.P., Erickson, M.R.S., Abmayr, S.M., 1999. Identification of a *Drosophila* homolog to vertebrate *crk* by interaction with MBC. Gene 228, 243–252.
Garen, A., Kauvar, L., Lepesant, J.A., 1977. Roles of ecdysone in Drosophila development. Proc. Natl. Acad. Sci. USA 74 (11), 5099–5103.
Gaul, U., Weigel, D., 1990. Regulation of Kruppel expression in the anlage of the Malpighian tubules in *Drosophila* embryo. Mech. Dev. 33, 57–67.
Gautam, N.K., Tapadia, M.G., 2010. Ecdysone signaling is required for proper organization and fluid secretion of stellate cells in the Malpighian tubules of *Drosophila melanogaster*. Int. J. Dev. Biol. 54, 635–642.
George, P.A., Michael, H.F., 1995. Intracellular Na^+ Measurements using sodium green tetraacetate with flow cytometry. Cytometry 21, 248–256.
Goldstein, J.I., et al., 2003. Scanning Electron Microscopy and X-ray Micronalysis, 3rd ed Plenum Press, New York.
Hall, A., 1998. Rho GTPases and the actin cytoskeleton. Science 279, 509–514.
Hasegawa, H., Kiyokawa, E., Tanaka, S., Nagashima, K., Gotoh, N., 1996. DOCK180, a major CRK-binding protein, alters cell morphology upon translocation to the cell membrane. Mol. Cell Biol. 16, 1770–1776.
Hatton-Ellis, E., Ainsworth, C., Sushama, Y., Wan, S., Raghavan, V.K., 2007. Genetic regulation of patterned tubular branching in *Drosophila*. Proc. Natl. Acad. Sci. USA 104, 1169–1174.
Harbeck, R., Langyel, J., 1995. Genes controlling posterior gut development in the *Drosophila* embryo. Roux's Arch. Dev. Biol. 204, 308–329.
Harbecke, R., Janning, W., 1989. The segmentation gene *Kruppel* of *Drosophila melanogaster* has homeotic properties. Genes Dev. 3, 114–122.
Henrich, V.C., Sliter, T.J., Lubahn, D.B., Macintyre, A., Gilbert, L.I., 1990. A steroid/thyroid hormone receptor superfamily member in *Drosophila melanogaster* that shares extensive sequence similarity with a mammalian homolog. Nucl. Acids Res. 18, 4143–4148.
Hirata, T., Cabrero, P., Berkholz, D.S., Bondeson, D.P., Ritman, E.L., 2012. In vovo Drosophilia genetic model for calcium oxalate nephrolithiasis. Am. J. Physiol. Renal. Physiol. 303, F1555–F1562.
Ianowski, J.P., O'Donnell, M.J., 2004. Basolateral ion transport mechanisms during fluid secretion by *Drosophila* Malpighian tubules: Na+ recycling, Na+:K+:2Cl- cotransport and Cl- conductance. J. Exp. Biol. 207, 2599–2609.
Janning, W., Lutz, A., Wissen, D., 1986. Clonal analysis of the blastoderm anlage of the Malpighain tubules in *Drosophila melanogaster*. Roux's Arch. Dev. Biol. 195, 22–32.
Jiang, C., Baehrecke, E.H., Thummel, C.S., 1997. Steroid regulated programmed cell death during *Drosophila* metamorphosis. Development 124, 4673–4683.
Jung, A., Denholm, B., Skaer, H., Affolter, M., 2005. Renal tubule development in *Drosophila*: a closer look at the cellular level. J. Am. Soc. Nephrol. 16, 322–328.
Kaufmann, N., Mathai, J.C., Hill, W.G., Dow, J.A.T., Zeidel, M.L., 2005. Developmental expression and biophysical characterization of a *Drosophila melanogaster* aquaporin. Am. J. Physiol. Cell Physiol. 289, 397–407.
Kiyokawa, E., Hashimoto, Y., Kurata, T., Sugimura, H., Matsuda, M., 1998. Evidence that DOCK180 up-regulates signals from the CrkII-p130 (Cas) complex. J. Biol. Chem. 273, 24479–24484.

Koelle, M.R., Toelle, M.R., Talbot, W.S., Segraves, W.A., Bender, M.T., 1991. The *Drosophila* EcR gene encodes an ecdysone receptor, a new member of the steroid receptor super family. Cell 67, 59–77.
Khoshnoodi, J., Tryggvason, K., 2001. Congenital nephrotic syndromes. Curr. Opin. Genet. Dev. 11, 322–327.
Lebovitz, R.M., Takeyasu, K., Fambrough, D.M., 1989. Molecular characterization and expression of the (Na^+/K^+)-ATPase -subunit in *Drosophila melanogaster*. EMBO 8, 193–202.
Schooley, D.A., Horodyski, F.M., Coast, G.M., 2012. Hormones controlling Homeostasis in insects. In: Lawrence I, Gilbert (Ed.), Insect Endocrinol. (P. 380).
Minta, A., Tsien, R.Y., 1989. Fluorescent indicators for cytosolic sodium. J. Biol. Chem. 264, 19449–19457.
Mouillet, J.F., Henrich, V.C., Lezzi, M., Vogtli, M., 2001. Differential control of gene activity by isoforms A, B1, and B2 of the *Drosophila* ecdysone receptor. Eur. J. Biochem. 268, 1811–1819.
Mlodzik, M., Hiromi, Y., Goodman, C.S., Rubin, G.M., 1990. The *Drosophila* seven-up gene, a member of the steroid receptor gene superfamily, controls photoreceptor cell fates. Cell 60, 211–224.
Nolan, K.M., Barrett, K., Lu, Y., Hu, K.Q., Vincent, S., 1998. Myoblast city, the *Drosophila* homolog of DOCK180/CED-5, is required in a Rac signaling pathway utilized for multiple developmental processes. Genes Dev. 12, 3337–3342.
O'Donnell, M.J., Spring, J.H., 2000. Patterns of control of insect Malpighian tubules: synergism, antagonism, cooperation and autonomous regulation. J. Insect Physiol. 46, 107–117.
O'Donnell, M.J., Dow, J.A.T., Huesmann, G.R., Tublitz, N.J., Maddrell, S.H.P., 1996. Separate control of anion and cation transport in Malpighian tubules of *Drosophila melanogaster*. J. Exp. Biol. 197, 421–428.
O'Donell, M.J., Rheault, M.R., Davies, S.A., Rosay, P., Harvey, B.J., 1998. Hormonally controlled chloride movement across *Drosophila* tubules is via ion channels in stellate cells. Am. J. Physiol. Regul. Integr. Comp. Physiol. 274, 1039–1049.
Oro, A.E., Mckeown, M., Evans, R.M., 1990. Relationship between the product of *Dosophila* ultraspiracle locus and vertebrate retinoid X receptor. Nature 347, 298–301.
Palladino, M.J., Bower, J.E., Kreber, R., Ganetzk, B., 2003. Neural dysfunction and neurodegeneration in *Drosophila* Na^+/K^+-ATPase alpha subunit mutants. J. Neurosci. 23 (4), 1276–1286.
Power, R.F., Lydon, J.P., Conneely, O.M., O'Malley, B.W., 1991. Dopamine activation of an orphan of the steroid receptor superfamily. Science 252, 1546–1548.
Putz, M., Kesper, D.A., Duttgereit, D., Renkawitz-pohl, R., 2005. In *Drosophila melanogaster*, the Rolling pebbles isoform 6 (Rols6) is essential for proper Malpighian tubule morphology. Mech. Dev. 122, 1206–1207.
Rosay, P., Davies, S.A., Yu, Y., Sozen, M.A., Kaiser, K., 1997. Cell-type specific calcium signaling in a *Drosophila* epithelium. J. Cell Sci. 110, 1683–1692.
Roy, M., Loukianova, E.S., Eberl, D.F., 2013. Cell-type-specific roles of Na^+/K^+ ATPase subunits in *Drosophila* auditory mechanosensation. PNAS 110, 181–186.
Schubiger, M., Wadea, A., Carney, G.E., Truman, J.W., Bender, M., 1998. *Drosophila* EcR-B ecdysone receptor isoforms are required for larval molting and for neuron remodeling during metamorphosis. Development 125, 2053–2062.
Shukla, A., Tapadia, M.G., 2011. Differential localization and processing of apoptotic proteins in Malpighian tubules of *Drosophila* during metamorphosis. Eur. J. Cell Biol. 90, 72–80.
Singh, S.R., Liu, W., Hou, S., 2007. The adult *Drosophila* Malpighian tubule are maintained by pluripotent stem cells. Cell Stem Cell. 16, 191–203.
Skaer, H., 1993. The alimentary canal. In: Bate, M., Arias, A.M. (Eds.), Development of *Drosophila melanogaster*. Cold Spring Harbor Laboratory Press, Plainview NY, pp. 941–1012.
Skaer, H., 1989. Cell division in Malpighian tubule development in *D. melanogaster* is regulated by a single tip cell. Nature 342, 566–569.
Smith, A.V., Orr-Weaver, T.L., 1991. Regulation of the cell cycle during *Drosophila* embryogenesis: the transition to polyteny. Development 112, 997–1008.
Sozen, M.A., Armstrong, J.D., Yang, M., Kaiser, K., Dow, J.A.T., 1997. Functional domains are specified to single cell resolution in a *Drosophila* epithelium. Proc. Natl. Acad. Sci. USA 94, 5207–5212.
Thomas, H.E., Stunnenberg, H.G., Stewart, A.F., 1993. Hetero dimerization of *Drosophila* ecdysone receptor with retinoid X receptor and ultraspiracle. Nature 362, 471–475.
Talbot, W.S., Swyryd, E.A., Hogness, D.S., 1993. *Drosophila* tissues with different metamorphic responses to ecdysone express different ecdysone receptor isoforms. Cell 73, 1323–1337.
Tapadia, M.G., Gautam, N.K., 2011. Non-apoptotic function of apoptotic proteins in the development of Malpighian tubules of *Drosophila melanogaster*. J. Biosci. 36, 531–544.
Thummel, C.S., 1995. From embryogenesis to metamorphosis: the regulation and function of *Drosophila* nuclear receptor superfamily members. Cell 83, 871–877.
Torrie, L.S., Radford, J.C., Southall, T.D., Kean, L., Dinsmore, A.J., Davies, A.S., 2004. Resolution of the insect ouabain paradox. PNAS 101 (37), 13689–13693.
Verma, P., Tapadia, M.G., 2012. Immune response and anti-microbial peptides expression in Malpighian tubules of *Drosophila* melanogaster is under developmental regulation. Plos One 7, e40714.
Verma, P., Tapadia, M.G., 2014. Epithelial immune response in *Drosophila* malpighian tubules: interplay between diap2 and ion channels. J. Cell Physiol. 229 (8), 1078–1095.
Wessing, A., Eichelberg, D., 1978. Malpighian tubules, rectal papillae and excretion. In: Ashburner, A., Wright, T.R.F. (Eds.), Genetics and Biology of *Drosophila*. London Academic Press, London, pp. 1–42.
Weigel, D., Bellen, H., Jurgens, G., Jackle, H., 1989. Primordeum specific requirement of the homeotic gene *fork head* in the developing gut of the *Drosophila* embryo. Roux's Arch. Dev. Biol. 98, 201–210.
Wigglesworth, V.B., 1965. The Principles of Insect Physiology, 6th edition Methuen, London.
Wu, L., Langyel, J., 1998. Role of caudal in hind gut specification and gastrulation suggests homology between *Drosophila* amnoproctodeal invagination and vertebrate blastopore. Development 125, 2433–2442.
Yao, T.P., Segraves, W.A., Oro, A.E., Mckeown, M., Evans, R.M., 1992. *Drosophila* ultraspiracle modulates ecdysone receptor function via heterodimer formation. Cell 71, 63–72.
Zelhof, A.C., Yao, T.P., Chen, J.D., Evans, R.M., McKeown, M., 1995. Seven-up inhibits ultraspiracle-based signaling pathways in vitro and in vivo. Mol. Cell Biol. 12, 6736–6745.